

Observation of pseudogap behaviour in a strongly interacting Fermi gas

J. P. Gaebler¹, J. T. Stewart¹, T. E. Drake¹, D. S. Jin^{1*}, A. Perali², P. Pieri² and G. C. Strinati²

Ultracold atomic Fermi gases present an opportunity to study strongly interacting fermionic systems in a controlled and uncomplicated setting. The ability to tune attractive interactions has led to the discovery of superfluidity in these systems with an extremely high transition temperature with respect to the Fermi temperature^{1,2} near $T/T_F = 0.2$. This superfluidity is the electrically neutral analogue of superconductivity; however, superfluidity in atomic Fermi gases occurs in the limit of strong interactions and defies a conventional Bardeen–Cooper–Schrieffer (BCS) description. For these strong interactions, it is predicted that the onset of pairing and superfluidity can occur at different temperatures^{3–5}. Thus, for a range of temperatures, a pseudogap region may exist, in which the system retains some of the characteristics of the superfluid phase—such as a BCS-like dispersion and a partially gapped density of states—but does not exhibit superfluidity. By making two independent measurements—the direct observation of pair condensation in momentum space and a measurement of the single-particle spectral function using an analogue to photoemission spectroscopy⁶—we directly probe the pseudogap phase. Our measurements reveal a BCS-like dispersion with back-bending near the Fermi wavevector k_F , which persists well above the transition temperature for pair condensation.

In conventional superconductors, fermion pairs and superconductivity appear simultaneously at T_c . The single-particle, or fermionic, excitation spectrum of a conventional superconductor follows a BCS dispersion given by

$$E_s = \mu \pm \sqrt{(\epsilon_k - \mu)^2 + \Delta^2} \quad (1)$$

where $\epsilon_k = \hbar^2 k^2 / 2m$, $\hbar = h / 2\pi$ and h is Planck's constant, k is the fermion wavevector, m is the fermion mass, μ is the chemical potential and Δ is the superfluid order parameter. The lower branch of the dispersion (minus sign in equation (1)), which is the occupied one at low temperature, has a positive slope at low momentum and then turns around and has a negative slope at high momentum. This 'back bending' behaviour arises because of the excitation gap and is a characteristic signature of superconductivity. In unconventional superconductors, such as high- T_c superconductors, this back-bending in the dispersion has been observed both below⁷ and, remarkably, above T_c (ref. 8). The observation of back-bending above T_c represents a pronounced departure from conventional BCS theory, which predicts that the normal state above T_c is a Fermi liquid with a monotonically increasing single-branch dispersion and a density of states that is smooth through the Fermi surface. The departure from a conventional BCS description above T_c in the form of a gapped excitation spectra is the essence of the pseudogap.

A satisfactory explanation of the origin and nature of the observed pseudogap phase in high- T_c superconductors has

remained elusive because of the complexity of the materials. In contrast, ultracold atomic gases are relatively free of complexity, for example, having no underlying lattice structure, impurities or domain boundaries. Moreover, the interactions responsible for pairing and superfluidity in ultracold atom gases are well understood at the few-body level. As a result, these systems are ideally suited for investigating the prediction of a pseudogap phase resulting from pre-formed pairs. There is much scientific literature on the topic of the pseudogap in strongly interacting atom gases with wide-ranging viewpoints and conclusions^{3–5,9–17}, including a recent article that predicts no pseudogap phase at all¹⁸. In some theories, the pseudogap phase is predicted to have a BCS-like dispersion (equation (1)), but where Δ is no longer the superfluid order parameter but instead corresponds to an excitation gap resulting from the formation of incoherent pairs^{3,5,11–17}. However, for the atomic gases, there is not yet experimental data to establish the existence of a pseudogap phase and confirm its properties. Radiofrequency spectroscopy experiments that probe excitations have been carried out above and below the critical temperature^{19,20}, but their interpretation relies on assuming a specific dispersion relation and therefore they cannot be used to distinguish between a pseudogap and a normal phase^{13,18}.

The question is then, do we have the necessary measurement tools to look for pseudogap physics in the neutral atom gas system? To probe the defining properties of a pseudogap regime one needs both a measurement of the transition temperature as well as a probe of the single-particle excitation spectra. In the atomic gas system, the onset of the superfluid phase is clearly detected through the observation of momentum-space condensation of atom pairs²¹. To probe the single-particle excitation spectra, we use a technique (recently developed for atoms) that uses momentum-resolved radiofrequency spectroscopy to realize an analogue of photoemission spectroscopy⁶. Using these two measurements—the direct observation of pair condensation to determine T_c and momentum-resolved radiofrequency spectroscopy to probe the pairing gap—we can now explore the issue of the pseudogap in atomic systems. In this letter, we report that a BCS-like dispersion, with back-bending near k_F , indeed persists even for temperatures substantially above the measured critical temperature for superfluidity. For the atomic gas system, which is clean and simple in comparison with high- T_c materials, this result provides evidence of a pseudogap region where incoherent pairs of correlated fermions exist above T_c .

To carry out these experiments, we cool a gas of fermionic ⁴⁰K atoms to quantum degeneracy in a far-detuned optical dipole trap as described in previous work⁶. We obtain a 50/50 mixture of atoms in two spin states, namely the $|f, m_f\rangle = |9/2, -9/2\rangle$ and $|9/2, -7/2\rangle$ states, where f is the total atomic spin and m_f is the projection along the magnetic-field axis. Our final stage of evaporation occurs at a magnetic field of 203.5 G, where the s -wave

¹JILA, National Institute of Standards and Technology (NIST) and University of Colorado, Department of Physics, University of Colorado, Boulder, Colorado 803090440, USA, ²Dipartimento di Fisica, Università di Camerino, I-62032 Camerino, Italy. *e-mail: jin@jilau1.colorado.edu.

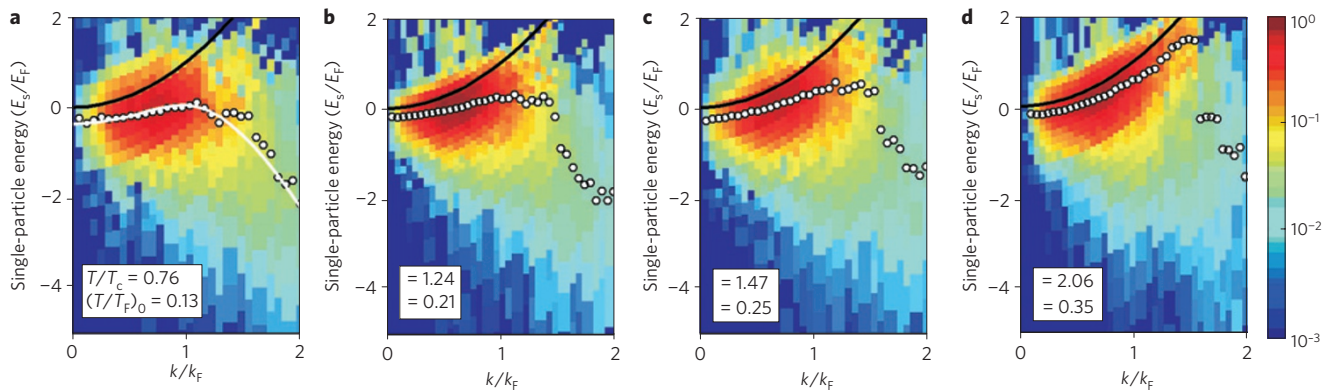


Figure 1 | Photoemission spectra throughout the pseudogap regime. Spectra for Fermi gases at four different temperatures, each with an interaction strength characterized by $(k_F a)^{-1} \approx 0.15$. The intensity plots show the fraction of out-coupled atoms as a function of their single-particle energy (normalized to E_F) and momentum (normalized to k_F), where $E = 0$ corresponds to a non-interacting particle at rest. The spectra are normalized so that integrating them over momentum and energy gives unity. The white dots indicate the centres extracted from Gaussian fits to individual EDCs (traces through the data at fixed momentum). The black curve is the quadratic dispersion expected for a free particle. **a**, At $T = 0.76 T_c$, we observe a BCS-like dispersion with back-bending, consistent with previous measurements⁶. The white curve is a fit to a BCS-like dispersion, equation (1). **b, c**, At $T = 1.24 T_c$ (**b**) and $T = 1.47 T_c$ (**c**), the dispersion with back-bending persists even though there is no longer any superfluidity. **d**, At $T = 2.06 T_c$, the dispersion does not exhibit back-bending in the range of $0 < k < 1.5 k_F$. In all of the plots there is a negative dispersion for $k/k_F > 1.5$. We attribute this weak feature (note the log scale) to a $1/k^4$ tail in the momentum distribution and not to the gap.

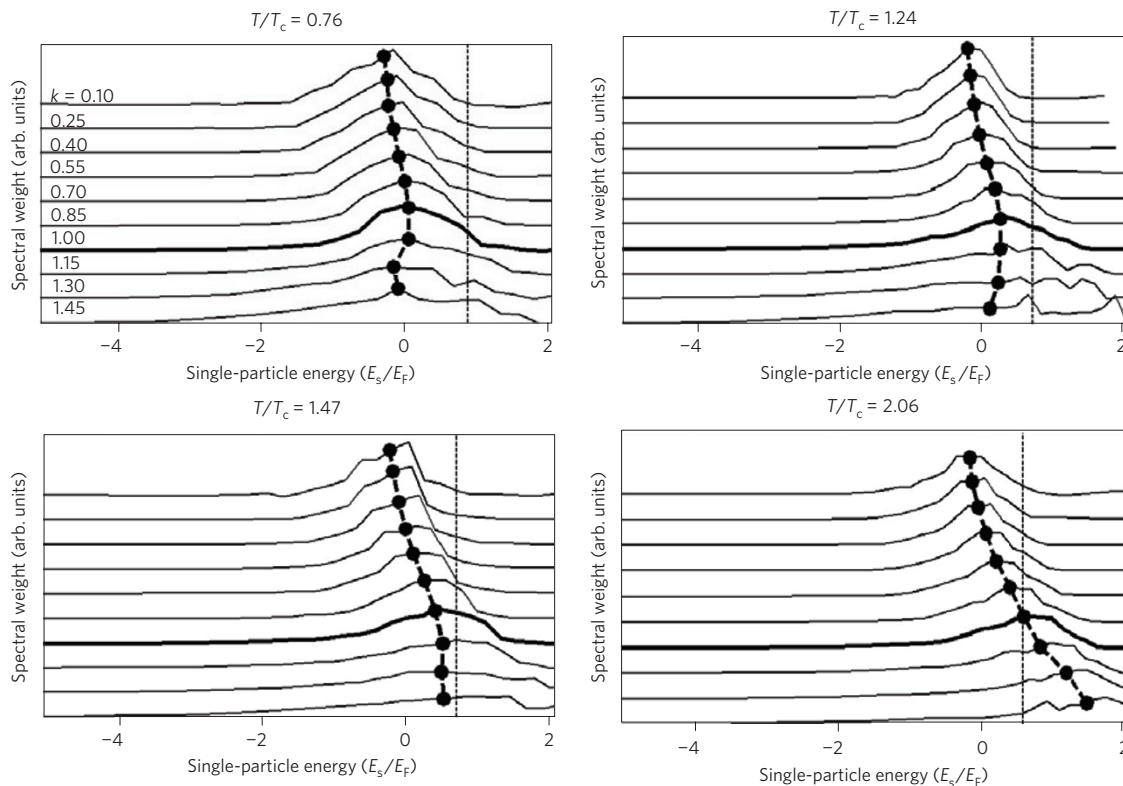


Figure 2 | EDCs. EDCs are obtained by taking vertical traces at fixed k through the photoemission spectra shown in Fig. 1. We show EDCs between $k/k_F = 0.1$ (top) and $k/k_F = 1.45$ (bottom) for the four data sets with T/T_c labelled above each panel. Each plotted EDC is an average of EDCs over a range of approximately $0.15 k_F$. The EDC at $k/k_F = 1.0$ is shown in bold. The black dots indicate the centres of the Gaussian fits to the EDCs. Each EDC is normalized to have an area of unity. The vertical dotted lines are placed at the local E_F that corresponds to the estimated average density of the gas.

scattering length that characterizes the interactions between atoms in the $|9/2, -9/2\rangle$ and $|9/2, -7/2\rangle$ states is approximately $800 a_0$, where a_0 is the Bohr radius. At the end of the evaporation we increase the interactions adiabatically with a slow magnetic-field ramp to a Feshbach scattering resonance.

To vary the temperature of the atom cloud, we either truncate the evaporation or parametrically heat the cloud by modulating

the optical dipole trap strength at twice the trapping frequency. To determine the temperature of the Fermi gas we expand the weakly interacting gas and fit the momentum distribution to the expected two-dimensional distribution¹ and extract $(T/T_F)_0$, where the subscript zero indicates a measurement made in the weakly interacting regime, before ramping the magnetic field to the Feshbach resonance. For the data presented here, we obtain clouds

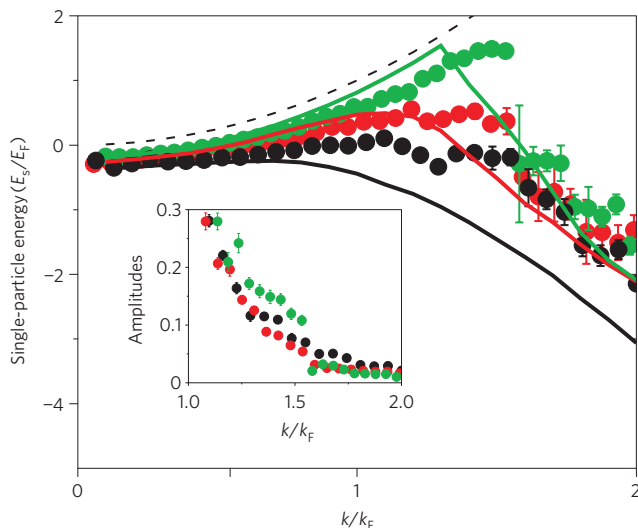


Figure 3 | Single-particle dispersion curves. The fits to the EDC centres for the three temperatures in Figs 1 and 2a,c and d, represented by black, red and green, respectively. We observe a BCS-like dispersion, smooth back-bending near $k/k_F = 1$, for temperatures below and moderately above T_c . For the highest temperature, we observe a quadratic dispersion near $k/k_F = 1$ and a sharp discontinuity near $k/k_F = 1.5$. The lines are theoretical curves that include effects of the harmonic trap and contact interaction, as described in the text. The error bars on the points represent one standard deviation of uncertainty from our fits. Inset: The amplitudes from the Gaussian fits to the EDCs for the same experimental data. The fit amplitudes evolve smoothly for the lower temperatures but jump discontinuously for the highest-temperature gas.

at final temperatures ranging from $(T/T_F)_0 = 0.12$ to 0.43 with $N = 1 \times 10^5 - 1.8 \times 10^5$ atoms per spin state. The trap frequencies vary depending on the final intensity of the optical trap and range from 180 to 320 Hz in the radial direction and 18 to 27 Hz in the axial direction. Correspondingly, the Fermi energy, E_F , ranges from $\hbar \cdot 8$ kHz to $\hbar \cdot 13$ kHz, where \hbar is Planck's constant. The Fermi energy is obtained from N and the geometric mean trap frequency, ν , as $E_F = \hbar\nu(6N)^{1/3}$. We define the Fermi wavevector as $k_F = \sqrt{2mE_F}/\hbar$ and the Fermi temperature as $T_F = E_F/k_B$, where k_B is the Boltzmann constant. It is important to note that the trapped gas has a spatially inhomogeneous density, and one can define a local Fermi energy, and corresponding local Fermi wavevector, that varies across the cloud.

Momentum-resolved radiofrequency spectroscopy realizes photoemission spectroscopy for strongly interacting atoms^{6,22}, much like angle-resolved photoemission spectroscopy (ARPES) for strongly correlated electron systems. In this spectroscopy, a radiofrequency photon flips the spin of an atom to a third hyperfine spin state and then the spin-flipped atoms are counted as a function of their momentum. As in ARPES (ref. 7), conservation of energy and momentum are used to extract the energy and momentum of the fermion (which in our case is an entire atom) in the strongly correlated system. A key feature of this measurement is that the spin-flipped atoms are 'ejected' from the system in the sense that they have only very weak interactions with the other atoms. This means that the spin-flipped atoms have the usual free-particle dispersion, and moreover, their momentum distribution can be measured using time-of-flight absorption imaging with no significant effects of interactions or collisions on the ballistic expansion. This technique was recently applied to a gas just below T_c and revealed a BCS-like back-bending dispersion characteristic of an excitation gap⁶.

To carry out the photoemission experiments on atoms, we turn on a short radiofrequency pulse to transfer atoms from

the $|9/2, -7/2\rangle$ state to the unoccupied and weakly interacting $|9/2, -5/2\rangle$ state. We then immediately turn off the trap and state-selectively image the out-coupled atoms on a CCD (charge-coupled device) camera after time-of-flight expansion. The radiofrequency pulse is kept much shorter than a trap period to ensure that the momentum of the out-coupled atoms does not change. The length of the radiofrequency pulse limits our energy resolution to approximately $0.2E_F$. As described in our previous work, the intensity of atoms out-coupled as a function of momentum for each radiofrequency can be used to reconstruct the occupied single-particle states⁶. With this information, one can determine the occupied part of the Fermi spectral function and probe the energy dispersion. It is important to note that unlike ARPES experiments in condensed-matter physics, the value of the chemical potential is not determined in this experiment. Rather, in our plots zero energy corresponds to the energy of a non-interacting atom at rest.

We present our photoemission spectroscopy data studying the pseudogap of a strongly interacting Fermi gas in Figs 1 and 2. The dimensionless parameter that characterizes the interaction strength for this data is $1/k_F a = 0.15(3)$, where a is the s -wave scattering length. In Fig. 1, we plot the fraction of out-coupled atoms as a function of their single-particle energy and momentum for temperatures encompassing the pseudogap regime. In the intensity plots, the white dots indicate the centres derived from unweighted Gaussian fits to each of the energy distribution curves (EDCs) (vertical trace at a given wavevector). The energy dispersion mapped out with these fits (white dots) can be contrasted to the expected free-particle dispersion for an ideal Fermi gas (black curve). In Fig. 2 we show the same data plotted as EDCs for wavevectors ranging from $k/k_F = 0.1$ to $k/k_F = 1.45$. To show the evolution of the spectral function from below T_c through the pseudogap regime the data are shown for four temperatures, $(T/T_F)_0 = 0.13, 0.21, 0.25$ and 0.35 .

For the data below T_c (Fig. 1a), we see a smooth back-bending that occurs near $k = k_F$. The white curve in Fig. 1a shows a BCS-like dispersion curve, equation (1), discussed above; here, we fit to the white dots for momenta in the range $0 < k < 1.4k_F$. Although we cannot use this fit to extract the gap and chemical potential in a model-independent way because of the harmonic trapping confinement, the BCS-like fit is consistent with a large pairing gap, of the order of E_F , as expected for a Fermi gas near the centre of the BCS to Bose–Einstein condensate (BEC) crossover^{1,2}.

In all four of our data sets in Fig. 1, we observe a weak signal with a strong negative dispersion at high momenta. It has been recently pointed out that one expects universal behaviour at $k \gg k_F$ for a Fermi gas with short-range, or contact, interactions²³, and, moreover, that this will give rise to a weak, negatively dispersing feature in the Fermi spectral function²⁴. Recently, we have directly verified this universal behaviour with measurements of the momentum distribution and found empirically that the expected $1/k^4$ tail occurs for $k > 1.5k_F$ (ref. 25). Therefore, we attribute the negative dispersion seen at large k to this universal behaviour for contact interactions. Although the strength of this feature should reflect the state of the system, the negative dispersion for $k > 1.5k_F$ does not, by itself, provide evidence of a BCS-pairing gap²⁴.

In the case of a pairing gap, we expect the spectral function to exhibit back-bending for k near k_F . To avoid effects of the universal behaviour at large k , we consider the spectral function for $k < 1.5k_F$. For the three lowest temperatures, we observe a BCS-like dispersion with back-bending behaviour that occurs near $k/k_F = 1$. In fact, we observe no qualitative change from the data at $T/T_c = 0.76$ to the data at $T/T_c = 1.24$. We interpret this as evidence for the existence of a pseudogap regime above T_c comprising uncondensed pairs in the strongly interacting Fermi gas. At our highest temperatures, $(T/T_F)_0 = 0.35$, the centres of the Gaussian fits to the EDCs increase quadratically through the region near $k/k_F = 1$ and then jump

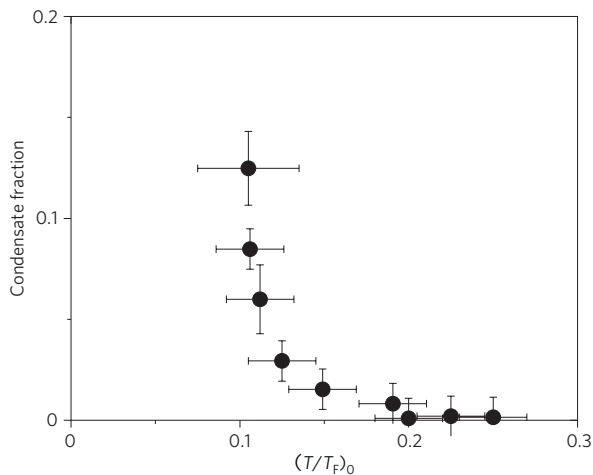


Figure 4 | Condensate fraction as a function of temperature. Using time-of-flight expansion at $B = 202.1$ G where our photoemission experiments are carried out, we map out the condensate fraction. Temperature is measured in the weakly interacting regime before the adiabatic ramp to strong interactions. We find $(T_c/T_F)_0 = 0.17 \pm 0.02$. Note that the density of the trapped cloud decreases with increasing distance from the trap centre, and therefore, in a local density picture, even at $T/T_F = 0.17$ only the part of the gas at the very centre of the trap is below T_c . The horizontal error bars represent one standard deviation of systematic uncertainty in the temperature and the vertical error bars represent a standard deviation of statistical error in the measurements.

discontinuously near $k/k_F = 1.5$. At the same point, the amplitudes of the fits also drop sharply (see inset to Fig. 3). Thus, we conclude that, as the occupation of the positively dispersing feature vanishes, the fits jump to a distinct, lower-energy feature in the spectral function. As discussed above, this lower-energy feature is consistent with the predicted effect of universal behaviour at large k on the spectral function²⁴.

In general, for data taken at finite temperature but still in the pseudogap regime one might expect to see population in the excited branch of the BCS Bogoliubov dispersion (plus sign in equation (1)). Signal in this branch represents thermally populated excitations above the pairing gap. The data in the region of $1 < k/k_F < 1.5$ are suggestive of some occupation in this branch. However, the limited signal-to-noise ratio makes it difficult to identify the excited branch in our data. In addition, the inhomogeneous density of the trapped gas could make the observation of two distinct branches more difficult. To be conservative, we fit each of the EDCs to a single Gaussian, and we find this to be sufficient to identify back-bending. It will be a subject of further research to see whether the excited branch can be more clearly observed in a momentum-resolved atom photoemission measurement.

In Fig. 3, we directly contrast the dispersions obtained for temperatures $T/T_c = 0.76$, 1.47 and 2.06, shown in black, red and green, respectively. We compare the experimental dispersions (circles) to a BCS–BEC crossover theory described in ref. 5. To compare to the experimental data, we fit theoretical EDCs to single Gaussians to extract the centres; the results are shown as lines in Fig. 3. The theory incorporates the trapping confinement as well as the energy resolution resulting from the finite radiofrequency pulse duration. The theory, which gives the expected k^{-4} behaviour at high k for the momentum distribution, agrees qualitatively with the experimental data. Both experimental and theoretical dispersions show smooth BCS-like dispersions with back-bending near $k = k_F$ for temperatures up to $T/T_c = 1.47$. For $T/T_c = 2.06$, both the experiment and theory show a quadratic dispersion before the

signal decays around $k = 1.5 k_F$, leaving a much weaker negatively dispersing feature as predicted for a normal gas with contact interactions. The disagreement between theory and experiment at $T/T_c = 0.76$ can be attributed to a sharp variation of the order parameter for temperature close to T_c . This may suggest the theory predicts too high an order parameter just below T_c . In the inset of Fig. 3, we show the amplitudes of the Gaussian fits to the measured EDCs for each of the three temperatures.

With theoretical calculations for a homogeneous Fermi gas, we find that the strongly interacting gas with pre-formed pairs and a normal Fermi liquid have distinct spectral functions. Namely, the paired state shows a smooth avoided crossing (such as described by equation (1)) whereas the normal Fermi liquid exhibits a sharp crossing leading to a cusp or apparent discontinuity in the occupied part of the spectral function. The smooth behaviour in the measured dispersion at the three lower temperatures, and the sharp jump in the dispersion at large k for the highest temperature data, are consistent with this theoretical picture.

To determine T_c , we probe pair condensation in our atomic Fermi gas following the procedure introduced in ref. 21. This technique directly probes coherence and has been used to map out T_c as a function of temperature and interaction strength²¹. The fact that the Bose condensation of fermion pairs corresponds to a superfluid phase transition was demonstrated unambiguously with the observation of a vortex lattice in a rotated Fermi gas below T_c (ref. 26). In addition, the accuracy of the condensate fraction measurements has been investigated both theoretically^{27,28} and experimentally²⁹. In Fig. 4, we show the measured pair condensate fraction as a function of the initial temperature of the Fermi gas. As an empirical definition of T_c , we use the temperature where the measured condensate fraction is 1%. The value of 1% is chosen because, when testing our fits with simulated data, we find that we cannot differentiate between a Bose distribution above T_c and one with a 1% condensate fraction. We find $(T_c/T_F)_0 = (0.17 \pm 0.02)$ at $1/k_F a = 0.15(3)$, and using this we report T/T_c for our photoemission spectroscopy data.

Contrasting the photoemission spectroscopy data with this direct measure of the temperature T_c below which the system has coherent pairs, we find that BCS-like back-bending persists well above T_c in what we identify to be the pseudogap phase. Above the superfluid transition temperature, these strongly interacting Fermi gases are clearly not described by a Fermi-liquid dispersion and the existence of many-body pairing well above T_c marks a significant departure from conventional BCS theory. It is intriguing to note that our measurements are qualitatively similar to ARPES results in high- T_c superconductors⁸, even though the atomic Fermi gas is a much simpler system that does not even have an underlying lattice structure. However, high- T_c materials and ultracold atom systems differ substantially and for example it may be important to consider that the atomic Fermi gas superfluids have a higher T_c/T_F compared with high- T_c superconductors and are more clearly in the region of the BCS–BEC crossover.

Methods

Feshbach resonance location. To create a strongly interacting gas we ramp the magnetic field after evaporation to a value of 202.1 G at an inverse ramp rate of 14 ms G^{-1} . The data presented here are at the same magnetic field as previous ‘on resonance’ results presented in Fig. 3b of ref. 6, where the value of a was based on a measurement of the resonance position in ref. 21. However, from a new measurement based on molecule binding energies determined from radiofrequency spectra, we find the resonance position to be $B_0 = 202.20(2)$ G and width to be $w = 7.1(2)$ G. With the new resonance parameters and $B = 202.1$ G, we find that the characteristic dimensionless interaction parameter $1/k_F a$ is $0.15(3)$. This corresponds to the region of the BCS–BEC crossover where the gas is extremely strongly interacting and the superfluid gap is expected to be of the order of E_F . Note that in the absence of many-body physics, the two-body prediction of the molecule binding energy at 202.1 G is 480 Hz, which is less than $0.05 E_F$.

Photoemission spectroscopy. For the work presented here, we have improved the signal-to-noise ratio of the photoemission spectra by a factor of four compared with our previous measurement⁶. Previously, a limitation to the signal-to-noise was related to imaging the out-coupled $|9/2, -5/2\rangle$ atoms, which lack a closed cycling transition for absorption imaging. Now, we transfer the out-coupled atoms to the $|9/2, -9/2\rangle$ state with two radiofrequency π -pulses. As the number of atoms in the $|9/2, -5/2\rangle$ state is relatively small, this requires that we first optically pump the atoms remaining in the $|9/2, -7/2\rangle$ and $|9/2, -9/2\rangle$ states to another hyperfine manifold. In this way, we can image the out-coupled atoms with the cycling transition for the $|9/2, -9/2\rangle$ state without contamination from the much larger population of atoms that were unaffected by the radiofrequency spectroscopy. Before constructing the photoemission spectra, we clean up the raw images by setting to zero data at large radii where the signal drops below technical noise.

Density inhomogeneity of the trapped gas. One can define a local Fermi energy, and corresponding local Fermi wavevector, that varies across the cloud. We can estimate the average density of the strongly interacting gas by taking the average density of an ideal trapped Fermi gas at a particular T/T_F and multiplying by $(E_{\text{pot}}/E_{\text{pot}}^0)^{-3/2}$. Here, $E_{\text{pot}}/E_{\text{pot}}^0$ is the measured ratio (at finite T) of the potential energy of the strongly interacting gas to that of a non-interacting gas³⁰. For the data shown in Fig. 1a–d, the local Fermi energy, in units of the previously defined E_F , which corresponds to this average density is 0.81, 0.69, 0.62 and 0.53, respectively. The corresponding local Fermi wavevector, in units of k_F , is 0.90, 0.83, 0.79 and 0.73, respectively. To give a sense of the spread in the local Fermi energies, we note that for the ideal trapped Fermi gas, the ratio of the local Fermi energy at the average density to that at the cloud centre is approximately 0.6.

Received 30 December 2009; accepted 20 May 2010;
published online 4 July 2010

References

- Regal, C. A. & Jin, D. S. Experimental realization of the BCS–BEC crossover with a Fermi gas of atoms. *Adv. Atom. Mol. Opt. Phys.* **54**, 1–79 (2006).
- Ketterle, W. & Zwierlein, M. W. in *Proc. of the International School of Physics ‘Enrico Fermi’, Course CLXIV* (eds Inguscio, M., Ketterle, W. & Salomon, C.) 95–287 (IOS Press, 2008).
- Janko, B., Maly, J. & Levin, K. Pseudogap effects induced by resonant pair scattering. *Phys. Rev. B* **56**, R11407–R11410 (1997).
- Randeria, M. in *Proc. of the International School of Physics ‘Enrico Fermi’, Course CXXXVI* (eds Iadonisi, G., Schrieffer, J. R. & Chialfalo, M. L.) 115–139 (IOS Press, 1998).
- Perali, A., Pieri, P., Strinati, G. C. & Castellani, C. Pseudogap and spectral function from superconducting fluctuations to the bosonic limit. *Phys. Rev. B* **66**, 024510 (2002).
- Stewart, J. T., Gaebler, J. P. & Jin, D. S. Using photoemission spectroscopy to probe a strongly interacting Fermi gas. *Nature* **454**, 744–747 (2008).
- Damascelli, A. Probing the electronic structure of complex systems by ARPES. *Phys. Scr.* **T109**, 61–74 (2004).
- Kanigel, A. *et al.* Evidence for pairing above T_c from the dispersion in the pseudogap phase of cuprates. *Phys. Rev. Lett.* **101**, 137002 (2008).
- Randeria, M., Trivedi, N., Moreo, A. & Scalettar, R. T. Pairing and spin gap in the normal state of short coherence length superconductors. *Phys. Rev. Lett.* **69**, 2001–2004 (1992).
- Sá de Melo, C. A. R., Randeria, M. & Engelbrecht, J. R. Crossover from BCS to Bose superconductivity: Transition temperature and time-dependent Ginzburg–Landau theory. *Phys. Rev. Lett.* **71**, 3202–3205 (1993).
- Yanase, Y. & Yamada, K. Theory of pseudogap phenomena in high- T_c cuprates based on the strong coupling superconductivity. *J. Phys. Soc. Jpn* **68**, 2999–3015 (1999).
- Bruun, G. M. & Baym, G. Bragg spectroscopy of cold atomic Fermi gases. *Phys. Rev. A* **74**, 033623 (2006).
- Massignan, P., Bruun, G. M. & Stoof, H. T. C. Twin peaks in rf spectra of Fermi gases at unitarity. *Phys. Rev. A* **77**, 031601(R) (2008).
- Barnea, N. Superfluid to insulator phase transition in a unitary Fermi gas. *Phys. Rev. A* **78**, 053629 (2008).
- Magierski, P., Wlazłowski, G., Bulgac, A. & Drut, J. E. The finite temperature pairing gap of a unitary Fermi gas by quantum Monte Carlo. *Phys. Rev. Lett.* **103**, 210403 (2009).
- Chen, Q., He, Y., Chien, C. C. & Levin, K. Theory of radio frequency spectroscopy experiments in ultracold Fermi gases and their relation to photoemission experiments in the cuprates. *Rep. Prog. Phys.* **72**, 122501 (2009).
- Tsuchiya, S., Watanabe, R. & Ohashi, Y. Single-particle properties and pseudogap effects in the BCS–BEC crossover regime of an ultracold Fermi gas above T_c . *Phys. Rev. A* **80**, 033613 (2009).
- Hausmann, R., Punk, M. & Zwerger, W. Spectral functions and rf response of ultracold fermionic atoms. *Phys. Rev. A* **80**, 063612 (2009).
- Chin, C. *et al.* Observation of the pairing gap in a strongly interacting Fermi gas. *Science* **305**, 1128–1130 (2004).
- Schirotzek, A., Shin, Y., Schunck, C. H. & Ketterle, W. Determination of the superfluid gap in atomic Fermi gases by quasiparticle spectroscopy. *Phys. Rev. Lett.* **101**, 140403 (2008).
- Regal, C. A., Greiner, M. & Jin, D. S. Observation of resonance condensation of fermionic atom pairs. *Phys. Rev. Lett.* **92**, 040403 (2004).
- Chen, Q. & Levin, K. Probing the spectral function using momentum resolved radio frequency spectroscopy in trapped Fermi gases. *Phys. Rev. Lett.* **102**, 190402 (2009).
- Tan, S. Large momentum part of a strongly correlated Fermi gas. *Ann. Phys.* **323**, 2971–2986 (2008).
- Schneider, W. & Randeria, M. Universal short-distance structure of the single-particle spectral function of dilute Fermi gases. *Phys. Rev. A* **81**, 021601 (2010).
- Stewart, J. T., Gaebler, J. P., Drake, T. E. & Jin, D. S. Verification of universal relations in a strongly interacting Fermi gas. *Phys. Rev. Lett.* **104**, 235301 (2010).
- Zwierlein, M. W., Abo-Shaer, J. R., Schirotzek, A., Schunck, C. H. & Ketterle, W. Vortices and superfluidity in a strongly interacting Fermi gas. *Nature* **435**, 1047–1051 (2005).
- Perali, A., Pieri, P. & Strinati, G. C. Extracting the condensate density from projection experiments with Fermi gases. *Phys. Rev. Lett.* **95**, 010407 (2005).
- Matyjaśkiewicz, S., Szymańska, M. H. & Góral, K. Probing fermionic condensates by fast-sweep projection onto Feshbach molecules. *Phys. Rev. Lett.* **101**, 150410 (2008).
- Zwierlein, M. W., Schunck, C. H., Stan, C. A., Raupach, S. M. F. & Ketterle, W. Formation dynamics of a fermion pair condensate. *Phys. Rev. Lett.* **94**, 180401 (2005).
- Stewart, J. T., Gaebler, J. P., Regal, C. A. & Jin, D. S. Potential energy of a ^{40}K Fermi gas in the BCS–BEC crossover. *Phys. Rev. Lett.* **97**, 220406 (2006).

Acknowledgements

We acknowledge financial support from the NSF. We thank the JILA BEC group for discussions. D.S.J. acknowledges discussions with A. Kanigel at the Aspen Center for Physics.

Author contributions

J.P.G., J.T.S., T.E.D. and D.S.J. carried out the experiments and analysed the data. A.P., P.P. and G.C.S. carried out theoretical calculations.

Additional information

The authors declare no competing financial interests. Reprints and permissions information is available online at <http://npg.nature.com/reprintsandpermissions>. Correspondence and requests for materials should be addressed to D.S.J.